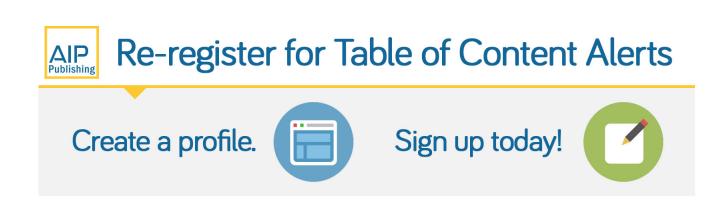# Aluminum Zintl anion moieties within sodium aluminum clusters

Haopeng Wang, Xinxing Zhang, Yeon Jae Ko, Andrej Grubisic, Xiang Li, Gerd Ganteför, Hansgeorg Schnöckel,

Bryan W. Eichhorn, Mal-Soon Lee, P. Jena, Anil K. Kandalam, Boggavarapu Kiran, and Kit H. Bowen

Aluminum Zintl anion moieties within sodium aluminum clusters

Haopeng Wang,[1] Xinxing Zhang,[1] Yeon Jae Ko,[1] Andrej Grubisic,[1] Xiang Li,[1]
Gerd Ganteför,[1] Hansgeorg Schnöckel,[2] Bryan W. Eichhorn,[3] Mal-Soon Lee,[4] P. Jena,[4]
Anil K. Kandalam,[5,a)] Boggavarapu Kiran,[6,a)] and Kit H. Bowen[1,a)]

[1]*Department of Chemistry, Johns Hopkins University, Baltimore, Maryland 21218, USA*
[2]*Institute of Inorganic Chemistry, Karlsruhe Institute of Technology, 76128 Karlsruhe, Germany*
[3]*Department of Chemistry, University of Maryland at College Park, College Park, Maryland 20742, USA*
[4]*Department of Physics, Virginia Commonwealth University, Richmond, Virginia 23284, USA*
[5]*Department of Physics, West Chester University of Pennsylvania, West Chester, Pennsylvania 19383, USA*
[6]*Department of Chemistry, McNeese State University, Lake Charles, Louisiana 70609, USA*

Through a synergetic combination of anion photoelectron spectroscopy and density functional theory based calculations, we have established that aluminum moieties within selected sodium-aluminum clusters are Zintl anions. Sodium–aluminum cluster anions, $Na_mAl_n^-$, were generated in a pulsed arc discharge source. After mass selection, their photoelectron spectra were measured by a magnetic bottle, electron energy analyzer. Calculations on a select sub-set of stoichiometries provided geometric structures and full charge analyses for both cluster anions and their neutral cluster counterparts, as well as photodetachment transition energies (stick spectra), and fragment molecular orbital based correlation diagrams. © 2014 AIP Publishing LLC. [http://dx.doi.org/10.1063/1.4862989]

I. INTRODUCTION

Zintl phases are typically solid state, salt-like A_aX_x compounds formed from electropositive elements, A, and somewhat electronegative main-group elements, X.[1,2] Zintl phases are differentiated from traditional inter-metallics and semiconductors by their salt-like character, i.e., A^+ and X^-, and the presence of substantial X–X bonding.[3] The prototypical Zintl phase, NaTl, is best described as a $(Na^+)(Tl^-)$ salt containing a $[Tl^-]$ network, where the thallium anions form a diamond lattice with direct Tl–Tl bonds.[4]

Zintl anions are multiply negatively charged polyatomic aggregates of main group elements and are often associated with the solution-based chemistry of naked clusters, e.g., Sn_5^{2-}, Sb_7^{3-}, Pb_9^{4-}, and Bi_4^{2-}.[5] As in Zintl phases, Zintl anions are also characterized by X–X bonding. In addition, Zintl anions often have "pseudo-atom" equivalents as described by Klemm.[6] For example, As_8^{8-} and Sb_8^{8-} are isoelectronic and isostructural to the S_8 rings in elemental sulfur.[7,8] Most Zintl anions display multi-center, multi-electron bonding, and they can be described by the electronic counting principles developed for the boron hydrides.[5] For example, Ge_9^{4-} and Pb_{10}^{2-} have *nido* and *closo* deltahedral structures,[9,10] respectively, as predicted from Wade's rules of electron counting. While Zintl anions are most commonly associated with the heavier main group elements (≥period 4), clusters of the 3rd period are also known, e.g., $Si_9^{3-/4-}$ and P_7^{3-}.[5,11,12]

Although most studies on Zintl anions have been conducted in condensed phases, there is also a growing body of work in the gas phase. There, Zintl anions occur as Zintl moieties within larger clusters, the net charge state of which is determined by the number of complementary cationic moieties present. For example, Zintl anions in clusters were first implicated in photoionization mass spectral studies of III–V and IV–V intermetallic clusters.[13] Additionally, the presence of the Bi_3^{3-} Zintl anion was inferred from the observation of $(Na_4Bi_3)^+$ as a magic number species in mass spectra.[13,14] The occurrence of the Zintl anions: Sn_4^{4-}, Ga_4^{2-}, Sn_{12}^{2-}, and Pb_{12}^{2-} within the cluster anions: $(Na_4Sn_4)^-$, $(NaGa_4)^-$, $(KSn_{12})^-$, and $(KPb_{12})^-$, respectively, has also been shown through the combination of anion photoelectron experiments and theoretical calculations.[15–18] Furthermore, the existence of Zintl anions in several endohedral cage clusters, such as $[M@Pb_{12}]^{2-}$ and $M@(Sn_{12})^-$, where M is a transition metal atom, has also been inferred.[19–22]

Interestingly, Zintl anions of aluminum have not been prepared in solution or solid phases. Although LiAl is isoelectronic and isostructural with the prototypical Zintl phase, NaTl, early theoretical studies showed limited charge transfer between lithium and aluminum, thus deviating from the traditional definition of a Zintl phase.[23–25] More recent studies, however, have shown substantial Al–Al interactions in an $[Al^-]$ network structure with bonding motifs that conform to the Zintl-Klemm concept of a Zintl phase.[3,26] Nevertheless, with few exceptions,[3,27] most solid compounds of aluminum with alkali metals have not been classified as Zintl phases.

In the condensed phase, aluminum clusters are more commonly found in the form of low oxidation state "metalloid clusters" as described by Schnoeckel.[28] While there are significant similarities between Zintl ions and metalloid clusters, there are defining differences as well. For example, Zintl ions are anionic and have elemental oxidation states of less than zero. In contrast, the metalloids contain elements with oxidation states greater than zero but less than the maximum valence state of the element. Nevertheless, while standalone aluminum Zintl anions are not known in condensed

---

a)Authors to whom correspondence should be addressed. Electronic addresses: AKandalam@wcupa.edu, kiran@mcneese.edu, and kbowen@jhu.edu

phases, aluminum Zintl anion subunits can be found in some metalloid clusters. The recently reported $[Al(O\text{-}t\text{-}Bu)_3]_6Al_6^{8-}$ metalloid[29] contains an Al_6^{8-} core that has Zintl-like characteristics, suggesting that substituted or stabilized aluminum Zintl clusters may be viable.

Further insight into the viability of aluminum Zintl cluster moieties can be gleaned through studies of aluminum-containing, gas phase clusters. Several such systems have already been examined both experimentally and theoretically. The aluminum cluster anion, Al_{13}^- has received substantial attention because of its unusual stability, which derives both from its electronic (a 40 valence electron shell closing) and its geometric structure (an icosahedron).[30,31] The ionic character of KAl_{13}, i.e., K^+ and Al_{13}^-, was theoretically predicted[32–34] and later experimentally confirmed by both photoionization[35,36] of KAl_{13} and anion photoelectron experiments[37,38] of $(KAl_{13})^-$. Although Al_{13}^- is not multiply charged and differs in that way from traditional Zintl anions, KAl_{13} can be seen as a 14-atom, "diatomic," ionic "molecule" and as such, as the basic unit of a hypothetical aluminum-based "Zintl phase." Cluster anions, $(LiAl_n)^-$ (n = 3–13) and $(CuAl_n)^-$ (n = 2–15), were also investigated by anion photoelectron spectroscopy, where interest in the formation of salt-like structures motivated those studies.[39,40] To further investigate their bonding motifs, studies of all-metal aromaticity (and anti-aromaticity) were also carried out on $(MAl_4)^-$ (where M = Li, Na, and Cu), on $(MAl_6)^-$ (where M = Li, Na, K, Cu, and Au), and on $(Li_3Al_4)^-$ cluster anions[41–43] by using a combination of anion photoelectron spectroscopy and theoretical calculations. Several mixed sodium–aluminum clusters and their anions were also studied through theoretical calculations.[44] Recently, the isolated, multiply charged aluminum cluster anions, Al_n^{2-} and Al_n^{3-}, were formed by electron attachment to gas phase, singly charged aluminum cluster anions in a Penning trap; there, the smallest observed sizes were n = 38 and 103, respectively.[45] Taken together, these experimental and computational studies of doped or pure aluminum clusters in gas phase have laid the foundation for exploring multiply charged, aluminum Zintl cluster anion moieties within larger clusters.

One can imagine a salt-like lattice made up of aluminum cluster anions and counter cations. Calculations, however, suggest that such a lattice, when composed of K^+ and Al_{13}^- ions, would not be stable.[33] On the other hand, if such a lattice were composed, not of singly charged aluminum cluster anions, but instead of multiply charged, aluminum cluster anions, i.e., aluminum Zintl anions, with an appropriate number of complementary cations, then a substantially greater lattice stabilization energy could be achieved. Under those circumstances, the formation of a bulk ionic material, i.e., a cluster-assembled material might be feasible. A first step in exploring this possibility involves assessing whether aluminum Zintl anion moieties can exist within mixed alkali metal–aluminum clusters.

Here, we present a combined experimental and theoretical study aimed at determining whether multiply charged, aluminum Zintl anionic moieties are formed within sodium–aluminum clusters. On the experimental side, anion photoelectron spectroscopic measurements were carried out on size-selected, sodium-doped aluminum cluster anions, $Na_mAl_n^-$. The results of these experiments pertain both to the anionic clusters and to their corresponding neutral clusters. To better understand the various properties of mixed sodium/aluminum clusters, calculations based on density functional theory (DFT) were also carried out both on the cluster anions and their neutral cluster counterparts. In addition to calculating photodetachment (photoelectron) transition energies for the cluster anions and geometric structures for both the cluster anions and their neutral counterparts, we also conducted full charge analyses through Natural Population Analysis (NPA), for both the cluster anions and their corresponding neutral clusters. Calculated photodetachment transition energies were compared with measured transitions in the photoelectron spectra. Geometric structures revealed the sub-structure of the aluminum cluster moieties and how the sodium atoms were arranged around them. Natural population analyses illuminated the extent of Zintl anion character in the aluminum moieties within these clusters. As such, NPA was our primary tool for identifying Zintl anion character in specific aluminum cluster moieties. Among the many sodium–aluminum cluster anions that we generated and studied by photoelectron spectroscopy, five stoichiometries and their neutral counterparts were selected to undergo the detailed theoretical analysis described above. These were $Na_2Al_6^-$, $Na_4Al_5^-$, $Na_5Al_5^-$, $Na_3Al_{12}^-$, and $Na_4Al_{12}^-$ as well as their neutral counterparts, Na_2Al_6, Na_4Al_5, Na_5Al_5, Na_3Al_{12}, and Na_4Al_{12}, respectively. These stoichiometries were chosen in part because they are all closed shell species[46] in either their anion or their neutral charge states. As closed shells, they would be expected to exhibit enhanced stability. The degree to which particular cluster stoichiometries conformed to the expectations of the shell model was explored through fragment molecular orbital (FMO) calculations and their resultant correlation diagrams.[47]

II. METHODS

A. Experimental

Anion photoelectron spectroscopy is conducted by crossing a mass-selected beam of negative ions with a fixed-frequency photon beam and energy-analyzing the resultant photodetached electrons. It is governed by the energy-conserving relationship, $h\nu = EBE + EKE$, where $h\nu$ is the photon energy, EBE is the electron binding (transition) energy, and EKE is the electron kinetic energy. Briefly, our apparatus, which has been described previously,[48] consists of a pulsed arc cluster ionization source (PACIS),[49] a time-of-flight mass spectrometer for mass analysis and mass selection, a Nd:YAG laser operated in these experiments at its third harmonic wavelength (355 nm, 3.49 eV/photon) for photodetachment, and a magnetic bottle, electron energy analyzer with a resolution of 30 meV at EKE = 1 eV. The photoelectron spectra were calibrated against the well-known photoelectron spectrum of Cu^-.[50]

In our pulsed arc cluster ionization source, a discharge is triggered between an anode and a grounded, conductive, sample cathode, while helium gas from a pulsed valve

is fed through the discharge region. In the present study, the sample cathode consists of an aluminum rod, with a cup-like depression on top, into which a mixture of aluminum powder and particles of sodium metal had been pressed into a disk. The sample material is vaporized by the discharge, cooled by the helium jet, and forms cluster anions as it travels down a 20 cm tube into high vacuum. The resulting cluster anions are then extracted, mass analyzed, and mass selected prior to being irradiated by photons.

B. Computational

Density functional theory based electronic structure calculations on Na_2Al_6, Na_4Al_5, Na_5Al_5, Na_3Al_{12}, and Na_4Al_{12} clusters and their anions were carried out using the Gaussian03 program.[51] The B3LYP functional form and the 6-311+G* basis set were used for all the calculations. The reliability of the theoretical method and the basis set used in this study had been established in a previous study on MAl_6^- (M = Li, Na, K, Cu, and Au) bi-metallic clusters.[42] During the geometry optimizations, the convergence criterion for energy was set to 10^{-9} hartree, while the gradient was converged to 10^{-4} hartree/Å. The vibrational frequencies of the reported isomers were calculated and found to be positive, indicating that these isomers are all minima on the potential energy surface. NPA, as implemented in the Gaussian03 code, were also carried out to determine the charge distributions in these clusters. The FMO of these five closed shell clusters were calculated at PW91/TZ2P using Amsterdam Density Functional Program.[52–54]

III. RESULTS AND DISCUSSION

The photoelectron spectra of all the $Na_mAl_n^-$ cluster anions measured in this study are presented in Figure 1. They were recorded using third harmonic (355 nm, 3.49 eV) photons from a Nd:YAG laser. The electron binding energies (EBE) of the peaks in each spectrum provide the photodetachment transition energies from the ground electronic state of the cluster anion to the ground and excited electronic states of the cluster anion's neutral counterpart. The EBE value near the onset (threshold) of the lowest EBE peak in a given photoelectron spectrum was taken as an estimate of the adiabatic electron affinity, EA, of the anion's neutral counterpart. The EBE value at the intensity maximum in the lowest EBE peak in the spectrum is the vertical detachment energy, VDE, which reflects the maximum Franck-Condon overlap between the wave functions of the anion's electronic ground state and the neutral's electronic ground state at the geometry of the anion.

Note that when neutral Na_mAl_n clusters exhibit closed electronic shell, with magic numbers of valence electrons, e.g., ... 8, 18, 20, 34, 40, 58 ..., the onset EBE values (estimated EA values) in their anions' photoelectron spectra tend to be smaller than those of their similar size neighbors. Additionally, the spacings between the lowest EBE and the next higher EBE peaks (the neutral clusters' HOMO-LUMO gaps) tend to be larger than those of their neighbors. On the other hand, when $Na_mAl_n^-$ cluster anions have closed electronic shell with magic number of valence electrons, their onset EBE values are higher than those of their similar size neighbors. In Figure 1, neutral closed shell Na_mAl_n clusters are marked with "**n**," while "**a**" closed shell $Na_mAl_n^-$ anions.
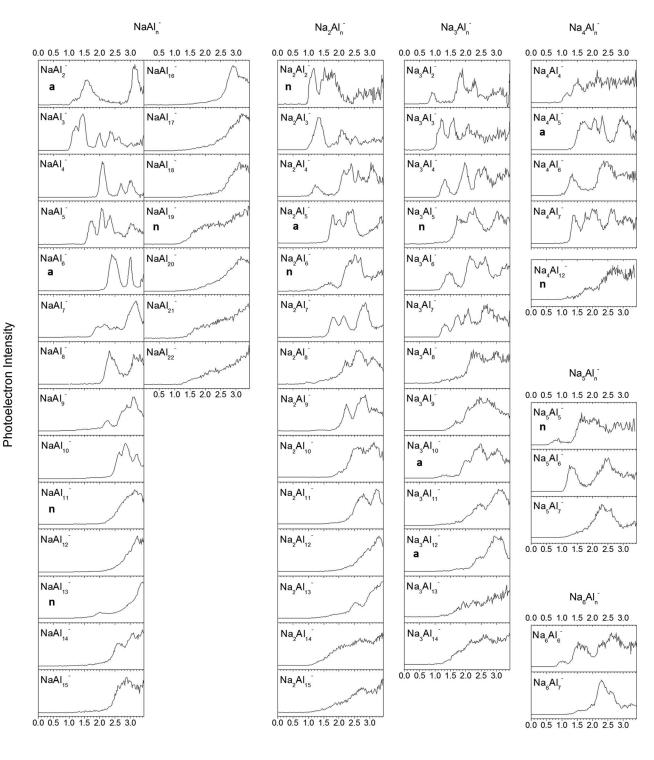
As described above, we have selected five of these $Na_mAl_n^-$ cluster anions and their neutral cluster counterparts for detailed computational scrutiny. These cluster anion/neutral cluster systems are: $Na_2Al_6^-/Na_2Al_6$, $Na_4Al_5^-/Na_4Al_5$, $Na_5Al_5^-/Na_5Al_5$, $Na_3Al_{12}^-/Na_3Al_{12}$, and $Na_4Al_{12}^-/Na_4Al_{12}$. Our calculations provided both the vertical detachment energy and the adiabatic detachment energy, ADE, for each of these anions, where ADE is the energy difference between the ground state geometry of the anionic cluster and the structurally similar/identical isomer (nearest local minimum) of its neutral counterpart. When the neutral and its anion have similar geometries, ADE = EA. Since our calculations show this structural similarity to be the case in the systems studied here, with the possible exception of the $Na_4Al_{12}^-/Na_4Al_{12}$ pair, the computed ADE value can be compared with the experimental EBE value at the spectral threshold, i.e., its estimated EA value. Table I presents both calculated and measured values of VDE and of ADE/EA.

Below, the five designated cluster anion/neutral cluster systems are presented and discussed in turn. In each case, we first present the calculated geometric structures of the lowest energy isomers of the cluster anion and its neutral cluster counterpart along with the natural population analysis for each structure. The extent of Zintl anion character in the aluminum moieties is then discussed in terms of their charge analyses. Next, we present the cluster anion's photoelectron spectrum along with its stick spectrum, the latter reflecting the calculated photodetachment transitions from the cluster anions' lowest energy isomers. Finally, we provide FMO correlation diagrams that support the closed electronic shell character of that particular cluster anion or its neutral counterpart.

A. $Na_2Al_6^-/Na_2Al_6$

Figure 2 presents the calculated structures of the three lowest energy isomers of $Na_2Al_6^-$ and Na_2Al_6 clusters. The most stable isomers, for both the anion and the neutral, are found to be Al_6 prisms with their two sodium atoms capping the faces of the two adjacent four-member rings (see structures, **1** and **4**). The structures of the second (**2** and **5**) and third (**3** and **6**) lowest energy isomers, which are 0.12 (0.10) eV and 0.16 (0.14) eV higher in energy than the corresponding lowest energy anion (neutral), are made up of Al_6 octahedra differing only in the positions of their sodium atoms over the surface of the cluster. Note that the Al_6 units (prism and octahedra) within the cluster anions are distorted relative to those within their corresponding neutral clusters. This is the result of the extra electron interacting with the Al_6 unit in each anionic isomer.

Since alkali metal atoms are significantly more electropositive than aluminum atoms, one might expect considerable charge transfer, formally 1*e*, from each sodium atom to the aluminum cluster moiety, leading to $(Na^+)_2(Al_6^{2-})$ in the

FIG. 1. Photoelectron spectra of $Na_mAl_n^-$ cluster anions, (m = 1, n = 2–22; m = 2, n = 2–15; m = 3, n = 2–14; m = 4, n = 4–7 and 12; m = 5, n = 5–7; m = 6, n = 6–7). Species with closed shell neutrals are marked by "**n**," and those with closed shell anions are marked by "**a**." Note that the valence electrons for these closed shell clusters, based on the jellium model, are 8, 18, 20, 34, 40, and 58.

case of the Na_2Al_6 neutral cluster. However, our NPA charge distribution analysis shows that a smaller amount of negative charge is actually transferred. In isomer **4**, both sodium atoms together donate $-1.54e$, instead of $-2.0e$, to Al_6 prism (see Figure 2). With a charge of $-1.54e$, we classify the Al_6 moiety as an incipient Zintl anion. In the case of the $Na_2Al_6^-$

cluster anion, where the net charge on the entire cluster is, by definition, $-1e$ and where the Al_6 moiety holds the lion's share of the negative charge ($-2.32e$ in isomer **1**), the two sodium atoms together contribute less negative charge to the aluminum moiety than they did in the case of the Na_2Al_6 neutral cluster. Interestingly, among the isomers of $Na_2Al_6^-$, as
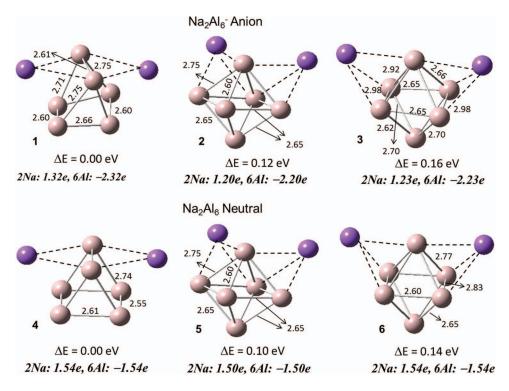
FIG. 2. The three lowest energy isomers of the $Na_2Al_6^-$ cluster anion and the Na_2Al_6 neutral cluster along with their relative energies, ΔE (eV). Isomers **1**–**3** correspond to the $Na_2Al_6^-$ anion, while **4**–**6** correspond to the lowest energy isomers of neutral Na_2Al_6. The gray spheres represent aluminum atoms and the purple spheres represent sodium atoms. All the bond lengths are given in Å. The calculated Natural Population Analysis (NPA) charges are given in italics below each isomer.

well as among those of Na_2Al_6, the extent of charge transfer to their respective Al_6 moieties is similar, even though the geometries of the Al_6 moieties vary from isomer to isomer.

Figure 3 presents the photoelectron spectrum of the $Na_2Al_6^-$ cluster anion. The first two photodetachment transitions have been calculated for each of the three lowest energy isomers of the $Na_2Al_6^-$ anion (**1**–**3**), and these are presented as stick spectra in Figure 3 (solid, dashed, and dotted sticks are for transitions from **1**, **2**, and **3**, respectively). Focusing on the lower energy transition, the calculated values of ADE and VDE for isomers **1** (1.20 eV and 1.63 eV), **2** (1.18 eV and 1.47 eV), and **3** (1.14 eV and 1.41 eV) compare well with the experimentally determined EA and VDE values of 1.20 and 1.66 eV, respectively (see Table I). Based on the calculated and measured values, it appears that all three anionic isomers may be present in the beam. Since neutral Na_2Al_6 is a closed

shell species (see below), the spacing between the first two transitions in the photoelectron spectrum provides its HOMO-LUMO gap. At ∼0.7 eV, this gap reflects the stability of neutral Na_2Al_6. Generally, the computational and experimental results are in good agreement.

Confirmation that the Na_2Al_6 neutral cluster, with its 20 valence electrons, exhibits electronic shell closure behavior is provided by its calculated FMO correlation diagram (see Figure 4). It shows that the levels group themselves into the

TABLE I. Experimental EA and theoretical ADE values of Na_2Al_6, Na_4Al_5, Na_5Al_5, Na_3Al_{12}, and Na_4Al_{12} neutral clusters and VDE values of $Na_2Al_6^-$, $Na_4Al_5^-$, $Na_5Al_5^-$, $Na_3Al_{12}^-$, and $Na_4Al_{12}^-$ cluster anions. All values are in eV. The calculated values for all low energy isomers are listed; the first listed value corresponds to the lowest energy isomer.

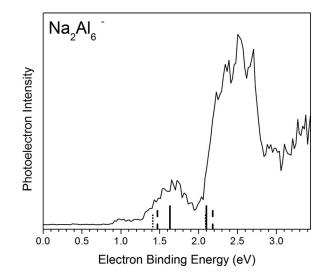| Cluster	ADE	EA	VDE	
	Theo.	Expt.	Theo.	Expt.
Na_2Al_6	1.20, 1.18, 1.14	1.20	1.63, 1.47, 1.41	1.66
Na_4Al_5	1.41, 1.68	1.44	1.52, 1.92	1.55
Na_5Al_5	0.64, 0.92	0.57	0.89, 1.02	0.87
Na_3Al_{12}	2.04	2.08	2.31	2.43
Na_4Al_{12}	1.21	1.45	1.88	1.89

FIG. 3. Photoelectron spectrum of the $Na_2Al_6^-$ cluster anion. The overlaid stick spectra indicate the calculated first two transitions from the $Na_2Al_6^-$ anion to its corresponding neutral cluster. (Solid sticks: isomer **1**; dashed sticks: isomer **2**; dotted sticks: isomer **3**.)
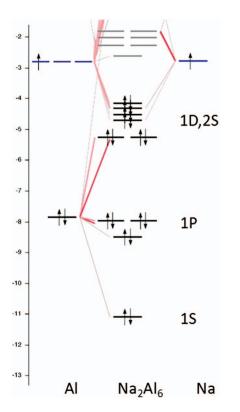
FIG. 4. The fragment molecular orbitals (FMO) analysis for the Na_2Al_6 neutral cluster.

1S, 1P, 1D/2S pattern expected under the jellium-like shell model[46] for free electron metals such as sodium and aluminum.

B. $Na_4Al_5^-$/Na_4Al_5

Figure 5 presents the computed structures of the two lowest energy isomers of $Na_4Al_5^-$ and Na_4Al_5 clusters. The lowest energy isomers of the $Na_4Al_5^-$ cluster anion, **7**, and the neutral Na_4Al_5 cluster, **9**, both adopt distorted octahedral-like structures, these being formed by an Al_5 square pyramid and a sodium atom occupying one of the vertices. The remaining three sodium atoms cap triangular faces. The second lowest energy isomers of the cluster anion, **8**, and the neutral cluster, **10**, are also both made up of Al_5 square pyramids. However, in each of these cases, all four of their sodium atoms bind to the base of their Al_5 square pyramids. Also, notice that while the energy difference between anion's two isomer structures is quite small (0.07 eV), the energy difference is significantly larger (0.35 eV) between the neutral's two isomer structures.

As in $Na_2Al_6^-$, the charge distributions in the isomers of the $Na_4Al_5^-$ cluster anion show that the majority of their excess electron resides on their aluminum moieties. Unlike $Na_2Al_6^-$, however, the net charge transfer in $Na_4Al_5^-$ to its Al_5 moiety differs considerably from isomer to isomer, with Al_5 in **7** receiving $-3.27 \, e$ but with Al_5 in **8** getting only $-2.51 \, e$. The difference may be due to the relatively symmetric location of the four sodium atoms around the Al_5 moiety in isomer **7**, compared with the asymmetric location of sodium atoms around this moiety in isomer **8**. In the case of the neutral Na_4Al_5 cluster, the charge distributions in isomers, **9** and
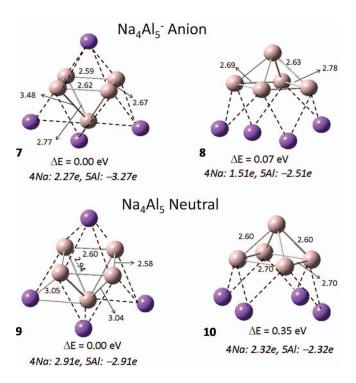

FIG. 5. The two lowest energy isomers of the $Na_4Al_5^-$ cluster anion and the Na_4Al_5 neutral cluster along with their relative energies, ΔE (eV). Isomers **7** and **8** correspond to the $Na_4Al_5^-$ cluster anion, while **9** and **10** correspond to the lowest energy isomers of the neutral Na_4Al_5 cluster. The gray spheres represent aluminum atoms and the purple spheres represent sodium atoms. All the bond lengths are given in Å. The calculated Natural Population Analysis (NPA) charges are given in italics below each isomer.

10, show that their Al_5 moieties possess net negative charges of about $-2.9 \, e$ and $-2.3 \, e$, respectively, this difference as well being influenced by the relative positions of the sodium atoms around the Al_5 moieties. These Al_5 aluminum moieties are clearly Zintl anions. A trend is emerging whereby multiply charged aluminum cluster moieties, i.e., aluminum Zintl anions, are more likely to form in sodium–aluminum clusters when several sodium atoms are available.

Figure 6 presents the photoelectron spectrum of the $Na_4Al_5^-$ cluster anion. The first few sets of photodetachment transitions have been calculated for each of the two lowest energy isomers of the $Na_4Al_5^-$ cluster anion (**7** and **8**), and these are presented as stick spectra in Figure 6 (solid and dashed sticks are for transitions from **7** and **8**, respectively). We have calculated ADE and VDE values for the lower energy transition in the cases of both isomer **7** and isomer **8** (see Table I). The VDE of **7** is 1.52 eV, and it matches well with the experimental value of 1.55 eV. On the other hand, the VDE of **8**, which is 1.92 eV, is significantly higher in energy than the observed value. The ADE values follow similar trends. The ADE of **7** is 1.41 eV, and this is close to the estimated value of 1.44 eV, whereas the ADE of **8** is 1.68 eV. Thus, it is likely that only isomer **7** is present in the cluster anion beam. Comparison of stick spectra for the two isomers with the experimental spectrum (see Figure 6) leads to the same conclusion.

In this system, the 20 valence electron, closed shell cluster is the $Na_4Al_5^-$ cluster anion. Figure 7 presents the calculated FMO correlation diagram for the $Na_4Al_5^-$ cluster anion. In a 20 valence electron cluster that obeys the jellium-like
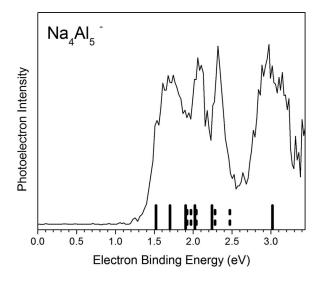
FIG. 6. Photoelectron spectrum of the $Na_4Al_5^-$ cluster anion. The overlaid stick spectra indicate the calculated low energy transitions from the $Na_4Al_5^-$ anion to its corresponding neutral cluster. (Solid sticks: isomer **7**; dashed sticks: isomer **8**.)

model, one would expect the $1S$ $1P$ $1D$ and $2S$ levels to be filled. It is evident from Figure 7 that the expected 20 valence electron, shell-closing is observed. The resulting MO energy levels form three distinct blocks, with the lowest two blocks corresponding to $1S$ and $1P$, and with the frontier block encompassing $1D$ and $2S$. Because the $Na_4Al_5^-$ cluster anion is a closed shell species, it would be expected to exhibit high
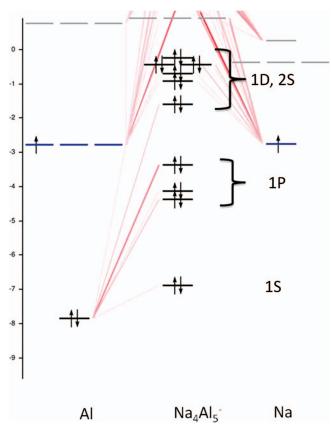

FIG. 7. The fragment molecular orbitals (FMO) analysis for the $Na_4Al_5^-$ cluster anion.
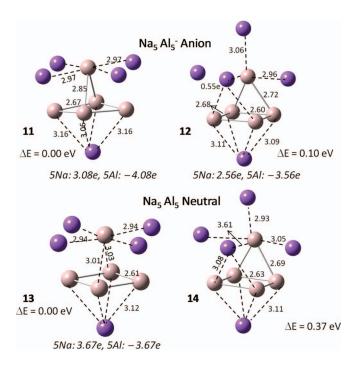

FIG. 8. The two lowest energy isomers of the $Na_5Al_5^-$ cluster anion and the Na_5Al_5 neutral cluster along with their relative energies, ΔE (eV). Isomers **11** and **12** correspond to the $Na_5Al_5^-$ anion, while **13** and **14** correspond to the lowest energy isomers of neutral Na_5Al_5. The gray spheres represent aluminum atoms and the purple spheres represent sodium atoms. All the bond lengths are given in Å. The calculated Natural Population Analysis (NPA) charges are given in italics below each isomer.

electron detachment energy. The fact that it does not may be due to excess negative charge accumulation on the Al_5 moiety, causing a destabilization of the frontier orbitals and thereby reducing the shell-closing effects in this system.

C. $Na_5Al_5^-/Na_5Al_5$

The calculated structures of the lowest energy isomers of the $Na_5Al_5^-$ cluster anion (**11** and **12**) and of the Na_5Al_5 neutral cluster (**13** and **14**) are presented in Figure 8. As in the $Na_4Al_5^-$ cluster anion and the Na_4Al_5 neutral cluster, the $NaAl_5$ sub-units in the lowest energy isomers of the $Na_5Al_5^-$ cluster anion (**11**) and the Na_5Al_5 neutral cluster (**13**) also adopt distorted octahedral geometries, with the remaining sodium atoms occupying various positions around this central core. Not surprisingly, the relative energies of the isomers of $Na_5Al_5^-$ and Na_5Al_5 are also similar to those of $Na_4Al_5^-$ and Na_4Al_5.

The $-3.67e$ charge on the Al_5 moiety of the Na_5Al_5 neutral cluster (structure **13**) shows that it is a Zintl anion. It is interesting to compare isoelectronic sodium/aluminum clusters, such as the $Na_4Al_5^-$ cluster anion and the Na_5Al_5 neutral cluster, where the additional sodium atom in Na_5Al_5 provides the extra negative charge (extra electron) in $Na_4Al_5^-$. In the $Na_4Al_5^-$ cluster anion (structure **7**), the net charge on the Al_5 moiety is $-3.27e$, whereas in the similarly structured Na_5Al_5 neutral cluster (structure **13**), it is $-3.67e$. The actual negative charges on the Al_5 moieties are comparable, regardless of the net charge state. Also, the net charge on the Al_5 moiety of the $Na_5Al_5^-$ cluster anion is $-4.08e$. The Al_5 moiety has
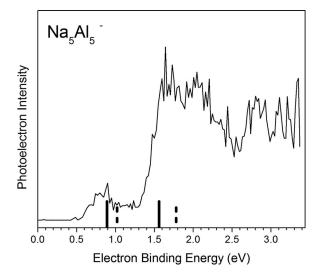
FIG. 9. Photoelectron spectrum of the $Na_5Al_5{}^-$ cluster anion. The overlaid stick spectra indicate the calculated first two transitions from the $Na_5Al_5{}^-$ cluster anion to its corresponding neutral cluster. (Solid sticks: isomer **11**; dashed sticks: isomer **12**.)

a propensity for forming Zintl anions when paired with five sodium atoms.

The photoelectron spectrum of the $Na_5Al_5{}^-$ cluster anion is presented in Figure 9. The first two photodetachment transitions have been calculated for each of the two lowest energy isomers of the $Na_5Al_5{}^-$ anion (**11** and **12**), and these are presented as stick spectra in Figure 9 (solid and dashed sticks are for transitions from **11** and **12**, respectively). We have calculated ADE and VDE values for the lower energy transition in the cases of both isomer **11** and isomer **12** (see Table I). The calculated VDE of **11** is 0.89 eV, and it compares well with the experimental value of 0.87 eV. On the other hand, the VDE of **12**, which is 1.02 eV, is significantly higher in energy than the observed value. The ADE values follow similar trends. The calculated ADE of **11** is 0.64 eV, and this is close to the estimated EA value of 0.57 eV, whereas the ADE of **12** is 0.92 eV. This suggests that only isomer **11** may be present in the cluster anion beam, although the stick spectra are consistent with both being present. Since the neutral Na_5Al_5 cluster is a 20 valence electron, closed shell species (see below), the spacing between the first two transitions in the photoelectron spectrum of the $Na_5Al_5{}^-$ cluster anion reflects the HOMO-LUMO gap of the neutral Na_5Al_5 cluster. At ∼0.7 eV, this gap reflects the stability of the closed shell Na_5Al_5 neutral cluster, just as it did in the case of neutral Na_2Al_6. The computational results show good agreement with the experimental photoelectron spectrum.

With 20 valence electrons, the Na_5Al_5 neutral cluster meets the condition for electronic shell closure. Figure 10 presents the calculated FMO correlation diagram for the Na_5Al_5 neutral cluster, where it exhibits three distinct blocks of MO energy levels, reflecting the 1S, 1P, 1D/2S pattern expected under the jellium-like model for a closed shell species. Not surprisingly, the isoelectronic species, $Na_4Al_5{}^-$ and Na_5Al_5 yield very similar, yet not identical FMO correlation diagrams (see Figures 7 and 10, respectively).
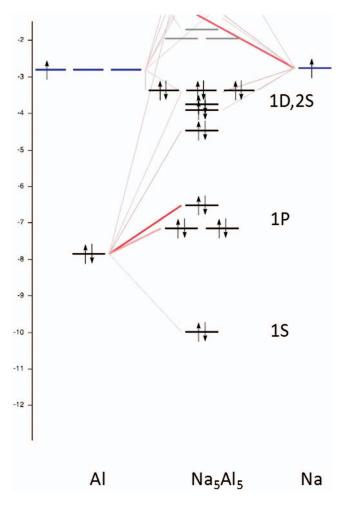

FIG. 10. The fragment molecular orbitals (FMO) analysis for the Na_5Al_5 neutral cluster.

D. $Na_3Al_{12}{}^-$/Na_3Al_{12}

Figure 11 presents the lowest energy structures of the $Na_3Al_{12}{}^-$ anion (**15**) and the Na_3Al_{12} neutral (**16**). Both of these exhibit rhombohedral-like structures, with an aluminum atom at the center, a sodium atom at one of the apexes, and the remaining two sodium atoms capping the two adjacent four-member rings. Other anion and neutral isomers of these clusters (not shown), where two sodium atoms cap two alternate four membered rings are also found to have energies which are close to those of the lowest energy structures. Substantial charge transfer to their Al_{12} moieties was found in both the $Na_3Al_{12}{}^-$ cluster anion ($-2.90e$) and in the Na_3Al_{12} neutral cluster ($-2.17e$). The Al_{12} moiety within the Na_3Al_{12} neutral cluster is a Zintl anion.

Figure 12 presents the photoelectron spectrum of the $Na_3Al_{12}{}^-$ cluster anion. The first photodetachment transition has been calculated for the lowest energy isomer of the $Na_3Al_{12}{}^-$ anion (**15**), and this is presented as a stick spectrum in Figure 12. We have calculated ADE and VDE values for this transition in the case of this isomer (see Table I). The calculated VDE is 2.31 eV, and it compares well with the experimental value of 2.43 eV. The calculated ADE is 2.04 eV, and this is close to the estimated EA value of 2.08 eV. The computational results show good agreement with the spectrum.
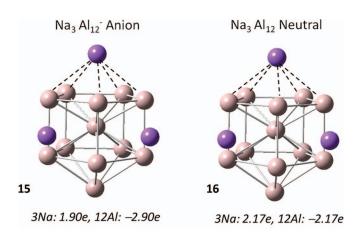
FIG. 11. The lowest energy isomers of the $Na_3Al_{12}^-$ cluster anion (**15**) and the Na_3Al_{12} neutral cluster (**16**). The gray spheres represent aluminum atoms and the purple spheres represent sodium atoms. The calculated Natural Population Analysis (NPA) charges are given in italics below each isomer.

The $Na_3Al_{12}^-$ cluster anion possesses 40 valence electrons, where 40, like 20, is an electronic shell closing, magic number. Figure 13 presents the calculated FMO correlation diagram for the $Na_3Al_{12}^-$ cluster anion. For 40 electrons, the expected filling order of the shells is $1S\ 1P\ 1D\ 2S\ 1F\ 2P$. As shown in Figure 13, the MO energy levels fall into four distinct blocks, corresponding to $(1S)$, $(1P)$, $(1D, 2S)$, and $(1F, 2P)$, thus supporting the expectation that the $Na_3Al_{12}^-$ cluster anion conforms to a 40 valence electron shell closure. Furthermore, because $Na_3Al_{12}^-$ is a closed shell species, it is expected to exhibit a relatively high electron affinity, and with ADE and estimated EA values of 2.04 eV and 2.08 eV, respectively, it does.

E. $Na_4Al_{12}^-/Na_4Al_{12}$

As shown in Figure 14, the $Na_4Al_{12}^-$ cluster anion adopts a capped icosahedral-like structure, with its missing ver-

FIG. 13. The fragment molecular orbitals (FMO) analysis for the $Na_3Al_{12}^-$ cluster anion.

tices occupied by sodium atoms (see structure **17**), while the Na_4Al_{12} neutral cluster exhibits a rhombohedral-like structure (see structure **18**). The structure of the latter is, in fact, quite similar to that of its isoelectronic counterpart, the $Na_3Al_{12}^-$ cluster anion, cf. structure **15**.

Charge analyses of the $Na_4Al_{12}^-$ cluster anion and the Na_4Al_{12} neutral cluster reveal net charges on their Al_{12} moieties of $-4.14e$ and $-3.43e$, respectively. Comparing the isoelectronic species, Na_4Al_{12} and $Na_3Al_{12}^-$, shows that the charges on their Al_{12} moieties are $-3.43e$ and $-2.90e$, respectively. It is interesting that the Al_{12} moiety within the Na_4Al_{12} neutral cluster possesses more negative charge than
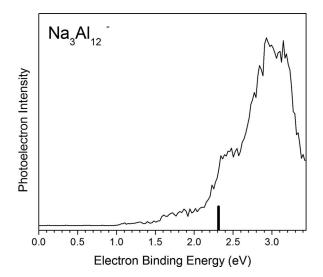

FIG. 12. Photoelectron spectrum of the $Na_3Al_{12}^-$ cluster anion. The overlaid stick spectra indicate the calculated transitions from the ground state of the $Na_3Al_{12}^-$ cluster anion to the ground state of the Na_3Al_{12} neutral cluster.
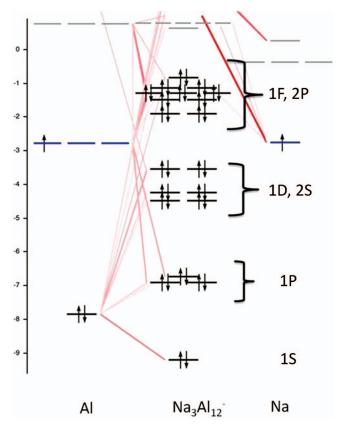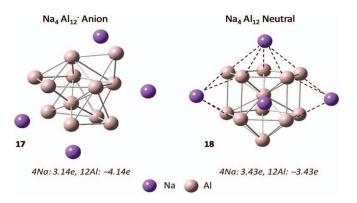

FIG. 14. The lowest energy isomers of the $Na_4Al_{12}^-$ cluster anion (**17**) and the Na_4Al_{12} neutral cluster (**18**). The gray spheres represent aluminum atoms and the purple spheres represent sodium atoms. The calculated Natural Population Analysis (NPA) charges are given in italics below each isomer.
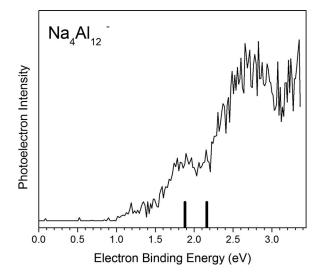
FIG. 15. Photoelectron spectrum of the $Na_4Al_{12}^-$ cluster anion. The overlaid stick spectra indicate the calculated transitions from the ground state of the $Na_4Al_{12}^-$ cluster anion to the ground and first excited states of the Na_4Al_{-12} neutral cluster.

the Al_{12} moiety within the $Na_3Al_{12}^-$ cluster anion. The Al_{12} moiety within the Na_4Al_{12} neutral cluster is a robust Zintl anion.

Figure 15 presents the photoelectron spectrum of $Na_4Al_{12}^-$ cluster anion. The first two photodetachment transitions have been calculated for the lowest energy isomer of the $Na_4Al_{12}^-$ anion, **17**, and these are presented as a stick spectrum in Figure 15. We have also calculated ADE and VDE values for the lower energy transition in the case of this isomer (see Table I). The calculated VDE is 1.88 eV, and it compares well with the experimental value of 1.89 eV. The calculated ADE is 1.21 eV, and this is in reasonable agreement with the estimated EA value of 1.45 eV. Since the Na_4Al_{12} neutral cluster is a 40 valence electron, closed shell species (see below), the spacing between the first two transitions in the photoelectron spectrum of the $Na_4Al_{12}^-$ cluster anion reflects the HOMO-LUMO gap of the neutral Na_4Al_{12} cluster. This computed HOMO-LUMO gap is ~0.3 eV. It reflects the enhanced stability of the closed shell Na_4Al_{12} neutral cluster, just as earlier discussed HOMO-LUMO gaps reflected the enhanced stabilities of the Na_2Al_6 and Na_5Al_5 neutral clusters. While the signal-to-noise ratio of the $Na_4Al_{12}^-$ cluster anion photoelectron spectrum leads to some degree of uncertainty, the calculated gap and observed spacing are broadly consistent.

The Na_4Al_{12} neutral cluster possesses 40 valence electrons, where 40 is a magic number. Figure 16 presents the calculated FMO correlation diagram for the Na_4Al_{12} neutral cluster. For 40 electrons, the expected filling order is $1S$ $1P$ $1D$ $2S$ $1F$ $2P$. As shown in Figure 16, the MO energy levels fall into four distinct blocks, corresponding to $(1S)$, $(1P)$, $(1D,$ $2S)$, and $(1F, 2P)$, thus supporting the expectation that the Na_4Al_{12} neutral cluster is a 40 valence electron closed shell species. Neutral Na_4Al_{12} is a geometrically symmetrical, energetically stabilized cluster that is home to an Al_{12} moiety with a negative charge of $-3.43e$, i.e., the multiply negatively charged Zintl anion, $Al_{12}^{3.43-}$.
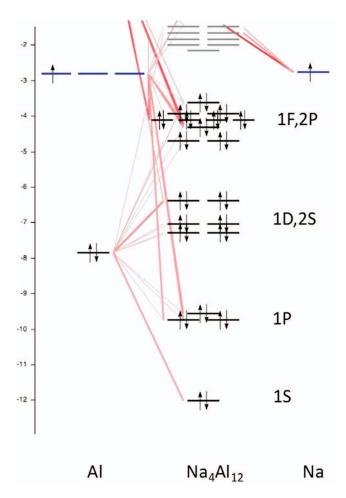

FIG. 16. The fragment molecular orbitals (FMO) analysis for the Na_4Al_{12} neutral cluster.

IV. CONCLUDING REMARKS

Through natural population (charge) analysis, we have established that the aluminum moieties within the sodium–aluminum clusters studied here are Zintl anions. Our computational results are validated by the good agreement between the values in Table I and between the computed stick spectra and their corresponding experimental photoelectron spectra. Roughly speaking, the charge on the aluminum moieties in the lowest energy isomers of both the neutral and the anionic sodium–aluminum clusters tends to be more negative for those clusters which possess larger numbers of sodium atoms. After all, sodium atoms are the primary sources of the electrons. Also, the differences between charges on the aluminum moieties in cluster anions and those on the aluminum moieties in their neutral cluster counterparts tend to be bigger, i.e., more negative, the larger the clusters' aluminum atom to sodium atom ratios. Furthermore, the charge distributions in sodium–aluminum cluster anions are consistent with those found in alkali and ammonium halide anions.[55, 56] In the latter cases, the halide anionic moieties, within the larger molecular anions, carry $-1e$ charge relative to their formally neutral alkali atom or ammonium radical partners. While the sodium moieties within sodium-aluminum cluster anions are not neutral and while their aluminum moieties carry more than one electron's worth of negative charge (they are Zintl anions),

the aluminum moieties nevertheless carry a net $-1e$ negative charge relative to their positively charged sodium moieties, just as in the anions of simpler salts.

A salt-like lattice made up of multiply charged, aluminum cluster anions, i.e., aluminum Zintl anions, and a charge-balancing number of counter-cations might be expected to achieve high lattice stabilization (cohesion) energy and with it, the potential of forming a bulk ionic (cluster-assembled) material. Although such materials would be metastable in a thermodynamic sense, they might nevertheless be stable on a practical time scale. As bulk materials, these compositions would carry an overall charge of zero. Thus, the basic units/building blocks of these materials would need to be uncharged as well. For this reason, the characterization of aluminum Zintl anions in *neutral* sodium–aluminum clusters has been our focus in this work. The neutral sodium–aluminum clusters are simply more relevant, than are sodium–aluminum cluster anions, for making a cluster-assembled material. Moreover, neutral sodium–aluminum clusters that also exhibit closed electronic shell would make, because of their enhanced stability, particularly promising candidates as building blocks of imagined bulk materials. The neutral clusters, Na_5Al_5 and Na_4Al_{12}, not only meet this condition, but with charges of -3.67 and -3.43, respectively, their aluminum moieties exhibit the highest negative charges seen in this work. These moieties are both robust aluminum Zintl anions.

Finally, two follow-on ideas come to mind. One involves utilizing more electropositive "atoms" than alkali metal atoms with which to form clusters with aluminum "Zintl" anions. Super-alkali molecules, such as Li_3O, are candidates.[57] Another approach is to make use of sodium–aluminum cluster anions as building blocks. After all, some of them are closed shell species, and strictly speaking, their aluminum moieties are also Zintl anions. The way to do this might be to form neutral salt clusters which are made up of alkali–aluminum cluster anions and electropositive atom cations, e.g., $Cu^+(Na_mAl_n)^-$, $Mg^{++}(Na_mAl_n)^=$, or $Li^+(Cs_mAl_n)^-$.

ACKNOWLEDGMENTS

[1]F. Laves, Naturwissenschaften **29**, 244 (1941).
[2]W. Klemm and E. Busmann, Z. Anorg. Allg. Chem. **319**, 297 (1963).
[3]*Zintl Ions: Principle and Recent Developments*, edited by T. F. Fassler (Springer-Verlag, Berlin, 2011).
[4]E. Zintl and W. Dullenkopf, Z. Phys. Chem. B **16**, 183 (1932).
[5]J. D. Corbett, Chem. Rev. **85**, 383 (1985).
[6]W. Klemm, Proc. Chem. Soc. **1958**, 329 (1958).
[7]H. G. von Schnering, J. Wolf, D. Weber, R. Ramirez, and T. Meyer, Angew. Chem., Int. Ed. Engl. **25**, 353 (1986).
[8]M. Reil and N. Korber, Z. Anorg. Allg. Chem. **633**, 1599 (2007).
[9]C. Suchentrunk, J. Daniels, M. Somer, W. Carrillo-Cabrera, and N. Korber, Z. Naturforsch. B **60**, 277 (2005).
[10]A. Spiekermann, S. D. Hoffmann, and T. F. Fassler, Angew. Chem., Int. Ed. Engl. **45**, 3459 (2006).
[11]V. Queneau, E. Todorov, and S. C. Sevov, J. Am. Chem. Soc. **120**, 3263 (1998).
[12]S. Joseph, C. Suchentrunk, F. Kraus, and N. Korber, Eur. J. Inorg. Chem. **2009**, 4641 (2009).
[13]R. W. Farley and A. W. Castleman, J. Am. Chem. Soc. **111**, 2734 (1989).
[14]R. W. Farley and A. W. Castleman, J. Chem. Phys. **92**, 1790 (1990).
[15]W. J. Zheng, O. C. Thomas, J. M. Nilles, K. H. Bowen, A. C. Reber, and S. N. Khanna, J. Chem. Phys. **134**, 224307 (2011).
[16]A. E. Kuznetsov, A. I. Boldyrev, X. Li, and L. S. Wang, J. Am. Chem. Soc. **123**, 8825 (2001).
[17]L. F. Cui, X. Huang, L. M. Wang, D. Y. Zubarev, A. I. Boldyrev, J. Li, and L. S. Wang, J. Am. Chem. Soc. **128**, 8390 (2006).
[18]L. F. Cui, X. Huang, L. M. Wang, J. Li, and L. S. Wang, J. Phys. Chem. A **110**, 10169 (2006).
[19]J.-P. Dognon, C. Clabaguera, and P. Pyykko, Angew. Chem., Int. Ed. **46**, 1427 (2007).
[20]A. Grubisic, H. Wang, X. Li, Y.-J. Ko, F. S. Kocak, M. R. Pederson, K. H. Bowen, and B. W. Eichhorn, Proc. Natl. Acad. Sci. U.S.A. **108**, 14757 (2011).
[21]L.-F. Cui, X. Huang, L.-M. Wang, J. Li, and L. S. Wang, Angew. Chem., Int. Ed. **46**, 742 (2007).
[22]U. Rohrmann, S. Schaefer, and R. Schaefer, J. Phys. Chem. A **113**, 12115 (2009).
[23]D. E. Ellis, G. A. Benesh, and E. Byrom, Phys. Rev. B **16**, 3308 (1977).
[24]A. Zunger, Phys. Rev. B **17**, 2582 (1978).
[25]K. Kishio and J. O. Brittain, J. Phys. Chem. Solids **40**, 933 (1979).
[26]N. E. Christensen, Phys. Rev. B **32**, 207 (1985).
[27]R. Nesper, Angew. Chem., Int. Ed. Engl. **30**, 789 (1991).
[28]A. Purath, R. Koppe, and H. Schnoeckel, Angew. Chem., Int. Ed. **38**, 2926 (1999).
[29]P. Henke, N. Trapp, C. E. Anson, and H. Schnoeckel, Angew. Chem., Int. Ed. **49**, 3146 (2010).
[30]R. E. Leuchtner, A. C. Harms, and A. W. Castleman, J. Chem. Phys. **94**, 1093 (1991).
[31]X. Li, H. Wu, X.-B. Wang, and L. S. Wang, Phys. Rev. Lett. **81**, 1909 (1998).
[32]S. N. Khanna and P. Jena, Phys. Rev. B **51**, 13705 (1995).
[33]F. Liu, M. Mostoller, T. Kaplan, S. N. Khanna, and P. Jena, Chem. Phys. Lett. **248**, 213 (1996).
[34]S. N. Khanna, B. K. Rao, and P. Jena, Phys. Rev. B **65**, 125105 (2002).
[35]A. Nakajima, K. Hoshino, T. Sugioka, T. Naganuma, T. Taguwa, Y. Yamada, K. Watanabe, and K. Kaya, J. Phys. Chem. **97**, 86 (1993).
[36]K. Hoshino, K. Watanabe, Y. Konishi, T. Taguwa, A. Nakajima, and K. Kaya, Chem. Phys. Lett. **231**, 499 (1994).
[37]W.-J. Zheng, O. C. Thomas, T. P. Lippa, S. J. Xu, and K. H. Bowen, J. Chem. Phys. **124**, 144304 (2006).
[38]Y. J. Ko, A. Shakya, H. Wang, A. Grubisic, W. Zheng, M. Goetz, G. Gantefoer, K. H. Bowen, P. Jena, and B. Kiran, J. Chem. Phys. **133**, 124308 (2010).
[39]O. C. Thomas, W.-J. Zheng, T. P. Lippa, S. J. Xu, and K. H. Bowen, J. Chem. Phys. **114**, 9895 (2001).
[40]O. C. Thomas, W.-J. Zheng, and K. H. Bowen, J. Chem. Phys. **114**, 5514 (2001).
[41]X. Li, A. E. Kuznetsov, H.-F. Zhang, A. I. Boldyrev, and L. S. Wang, Science **291**, 859 (2001).
[42]A. E. Kuznetsov, A. I. Boldyrev, H. J. Zhai, X. Li, and L. S. Wang, J. Am. Chem. Soc. **124**, 11791 (2002).
[43]A. E. Kuznetsov, K. A. Birch, A. I. Boldyrev, X. Li, H. J. Zhai, and L. S. Wang, Science **300**, 622 (2003).
[44]A. Dhavale, D. G. Kanhere, S. A. Blundell, and R. R. Zope, Phys. Rev. B **65**, 085402 (2002).
[45]N. Walsh, F. Martinez, G. Marx, and L. Schweikhard, Eur. Phys. J. D **43**, 241 (2007).

[46]W. D. Knight, K. Clemenger, W. A. de Heer, W. A. Saunders, M. Y. Chou, and M. L. Cohen, Phys. Rev. Lett. **52**, 2141 (1984).

[47]F. M. Bickelhaupt and E. J. Baerends, in *Reviews in Computational Chemistry*, edited by K. B. Lipowitz and D. B. Boyd (Wiley, New York, 2000), Vol. 15, pp. 1–86.

[48]M. Gerhards, O. C. Thomas, J. M. Nilles, W. J. Zheng, and K. H. Bowen, J. Chem. Phys. **116**, 10247 (2002).

[49]X. Li, A. Grubisic, S. T. Stokes, J. Cordes, G. F. Gantefoer, K. H. Bowen, B. Kiran, M. Willis, P. Jena, R. Burgert, and H. Schnoeckel, Science **315**, 356 (2007).

[50]J. Ho, K. M. Ervin, and W. C. Lineberger, J. Chem. Phys. **93**, 6987 (1990).

[51]M. J. Frisch, G. W. Trucks, H. B. Schlegel *et al.*, GAUSSIAN 03, Revision C.02, Gaussian, Inc., Wallingford, CT, 2004.

[52]G. te Velde, F. M. Bickelhaupt, S. J. A. van Gisbergen, C. Fonseca Guerra, E. J. Baerends, J. G. Snijders, and T. Ziegler, J. Comput. Chem. **22**, 931 (2001).

[53]C. Fonseca Guerra, J. G. Snijders, G. te Velde, and E. J. Baerends, Theor. Chem. Acc. **99**, 391 (1998).

[54]ADF2013, SCM, Theoretical Chemistry, Vrije Universiteit, Amsterdam, The Netherlands, http://www.scm.com.

[55]T. M. Miller, D. G. Leopold, K. K. Murray, and W. C. Lineberger, J. Chem. Phys. **85**, 2368 (1986).

[56]S. N. Eustis, D. Radisic, K. H. Bowen, R. A. Bachorz, M. Haranczyk, G. K. Schenter, and M. Gutowski, Science **319**, 936 (2008).

[57]D. Wang, J. D. Graham, A. M. Buytendyk, and K. H. Bowen, J. Chem. Phys. **135**, 164308 (2011).